ELSEVIER

Phororedox and photocatalytic processes on Fe(III)–porphyrin surface modified nanocrystalline TiO$_2$

A. Molinari [a], R. Amadelli [a, *], L. Antolini [a], A. Maldotti [a], P. Battioni [b], D. Mansuy [b]

[a] *Centro di Studio su Fotoreattività e Catalisi (CNR), Dipartimento di Chimica, Università di Ferrara, via L. Borsari, 46-44100 Ferrara, Italy*
[b] *Laboratoire de Chimie et Biochimie Pharmacologiques et Toxicologiques, URA 400 CNRS, Université René Descartes, 45 rue de Saints Pères, F-75270 Paris Cèdex 06, France*

Abstract

Surface derivatization of titanium dioxide nanoparticles with a Fe(III)–porphyrin has been carried out following a new procedure whereby the complex, rather than the surface, contains the aminopropylsilane functional group. This avoids the problems of surface deactivation by silane groups, reported in earlier investigations, on analogous systems. Characterization of the light-transparent dispersions by laser flash photolysis, UV-vis spectroscopy and photo-electrochemical methods has shown that the nature of the solvent is an important parameter in determining the redox processes involving the grafted porphyrin. In particular, one observes marked effects on the stability of the Fe(II)–porphyrin formed upon capture of the photogenerated electrons. The photocatalytic activity of the composite systems was assessed in the process of monooxygenation of cyclohexane and cyclohexene by molecular oxygen. The bonded porphyrin enhances the yield and the formation of the monooxygenation products with respect to total degradation to CO$_2$ for both the examined substrates. On this basis, we can claim an increase in the efficiency and selectivity with the composite photocatalytic system. In the case of cyclohexane, we observed, in addition, that the iron–porphyrin complex also changes the selectivity of the process, increasing the alcohol to ketone ratio. © 2000 Elsevier Science B.V. All rights reserved.

Keywords: TiO$_2$; Iron–porphyrin; Photocatalysis; Oxygen activation; Hydrocarbon oxidation

1. Introduction

Molecular modification of surfaces is a field of high interest in heterogeneous catalysis. A vast literature has emphasized the importance of the design and control of interfaces at a molecular resolution for the development of functional catalytic surfaces [1]. The structure of the surface plays a significant role in a wide range of applications, from synthesis to energy conversion, from sensor applications to pollution abatement.

Much work has been carried out on the modification of semiconductor surfaces for the improvement of stability and of charge separation. These investigations have provided an impetus to current studies on the use of semiconductors particularly as light-harvesting systems or as catalysts for pollution abatement. For energy

---

* Corresponding author. Tel.: +39-532-291-148; fax: +39-532-240-709.

conversion purposes, molecular modification of wide band gap semiconductors with dye sensitizers has long been known, and recent significant achievements have been reported [2]. In the field of photoelectrocatalysis, most of the reported studies are concerned with semiconductors modified by small metallic particles [3–6]. Less attention has seemingly been paid to molecular functionalized semiconductor surfaces for photoelectrosynthetic applications [7–22]. In this case, the aim is that of controlling the reactivity and selectivity of the semiconductor catalyst in a given process by linking it with non-light absorbing molecules. This strategy can potentially provide new contributions to the field of ''green chemical processes'' where one seeks a high selectivity under mild and environment-friendly conditions.

Titanium dioxide is one of the most suitable semiconductors for practical applications; however, the highly oxidizing conditions generated at the illuminated oxide surface place some limitations upon its use in photoelectrosynthetic oxidation processes since the desired products may undergo further oxidation and in extreme cases even total degradation [23].

Prior work by our group has shown that photocatalytic systems in which porphyrins are bonded to the surface of titanium dioxide show a new reactivity in the monooxygenation of alkanes [21,22]. We pointed out that this functionalization creates an ''integrated system'' where the solid support and the molecular component, taken separately, possess an individual catalytic activity. In homogeneous phase, the polyoxometallate/porphyrin integrated systems is another example where we could achieve significant benefits in the monooxygenation of hydrocarbons [24–26].

In our earlier work, the derivatization of TiO_2 with porphyrins was carried out in a two-step sequence [22]: triethoxypropylaminosilane was first grafted to the oxide surface and then the porphyrin was linked through the amino functional groups. In the first step, the surface suffers a drastic loss of activity, which is in part

recovered when the porphyrin is attached to the silane chains. Quite interestingly, however, this permitted the identification of the iron–porphyrin as the active reaction site.

Here, we report on a new functionalization procedure of TiO_2 in which an iron–porphyrin complex directly bears a silane chain that can be grafted to the surface. This reduces the ratio of silane groups per linked complex, in principle avoiding the deactivation of the surface sites not occupied by the bonded complex. We used a *meso*-tetraaryl iron–porphyrin bearing chlorine atoms in the *meso*-aryl groups able to provide a steric protection of the porphyrin ring against oxidative degradation [24–26].

We discuss the results of a characterization of the composite catalyst based on spectroscopic and photoelectrochemical measurements as well as on the assessment of its photocatalytic activity in the oxidation of hydrocarbons by molecular oxygen. We used colloidal TiO_2 for these studies because it is transparent enough to allow spectroscopic investigations to be performed and, at the same time, it can be conveniently deposited on inert substrates, such as glass, or on conductive electrodes.

2. Experimental

2.1. Synthesis and preparation of the colloidal composite system $TiO_2 / Fe(III)–porphyrin$

Colloidal TiO_2 was prepared following known procedures [27]. The precursor of the iron–porphyrin complex bearing a trifluorosilyl function to link to the surface of the semiconductor was the Fe(III)–*meso*-(tetrakis(2,6-dichlorophenyl)porphyrin (Fe(III)TDCPP). The silanization of this complex was not possible directly, as already reported for Fe(III)–*meso*-tetrakis(pentafluorophenyl)porphyrin, [28] but it has been necessary to modify the complex to introduce a good leaving group on the phenyl rings.

All the intermediates obtained during the preparation of the silanized Fe(III)–porphyrin

are reported in Scheme 1. The free porphyrin (**1**) was prepared following the method suggested by Lindsey et al. [29]: a 3-l one-neck flask was charged with CH_2Cl_2 (2.2 l distilled from CaH_2) and 2,6-dichlorobenzaldehyde (8 g, Acros) under an argon stream for 20 min. Then, pyrrole (3.3 g, Acros) and 2,2-dimethoxypropane (200 μl, Aldrich) were added. The reaction mixture was purged for an hour and added with three aliquots of Et_2OBF_3 (500 μl each, Aldrich) at 30-min intervals. After 24 h of rest, the formation of porphyrinogen was monitored by UV-vis absorption spectrophotometry (large and weak band at 512 nm). It is then oxidized by 2,3-dichloro-5,6-dicyano-1,4-benzoquinone (13 g, Aldrich) previously dissolved in toluene (400 ml, SDS). H_2TDCPP (**1**) was purified by column chromatography with neutral activated alumina (150 mesh, Aldrich) and CH_2Cl_2 as eluent, then concentrated, precipitated from *n*-pentane, dried at 100°C and characterized by UV-vis (418, 512 and 588 nm) and ^1H NMR [δ 8.64 (s, 8H, *H*-pyrrole), δ 7.72 (8H, *H-m*-phenyl), δ 7.19 (4H, *H-p*-phenyl), δ −2.54 (s, 2H, NH) in $CDCl_3$]. An aromatic electrophylic substitution reaction with $ClSO_3H$ (Janssen Chimica) on (**1**) under rigorously controlled conditions (100°C, 3 h) gave (**2**), which has been characterized by ^1H NMR [δ 8.62 (s, 8H, *H*-pyrrole), δ 8.60 (4H, *H-m*-

phenyl), δ 8.05 (4H, *H-p*-phenyl), δ −2.51 (s, 2H, NH) in $CDCl_3$]. Subsequent hydrolysis yielded (**3**) (IR: stretching frequency of SO_3H groups at 1190 and 1050 cm^{-1}).

An aqueous solution of $FeCl_2 \cdot 4H_2O$ (Janssen Chimica) was allowed to react with (**3**) under argon at 80°C for 18 h. The formation of the iron–porphyrin complex (**4**) was followed by UV-vis spectrophotometry (Soret band at 394 nm). After oxygenation of the sample, KOH (35%) was added until pH 8–9 to precipitate iron in excess as $Fe(OH)_3$. After filtration, the reaction mixture has been neutralized with HCl (35%) and the iron–porphyrin complex was purified by column chromatography with an ionic exchange resin (Dowex 50×8-200, Janssen Chimica). After concentration, it was then precipitated from acetone.

Chlorination was performed on the complex (**4**) (1 g) using PCl_5 (3.5 g) and $POCl_3$ (10 ml) at 50°C, for 30 min to lead to (**5**). Finally, this was a suitable complex for the nucleophilic substitution by excess aminopropyl triethoxysilane (aptes, 160 mg/50 mg of (**5**)) for 17 h under argon in the presence of pyridine (30 μl) in THF (4 ml) at 70°C. Unfortunately, the monomer (**6**) could not be directly removed from the reaction mixture because of a partial polymerization between the monomers and the excess nucleophilic reagent. A two-step purification process was devised: (i) hydrolysis and polycondensation of the crude mixture; and (ii) treatment with HF (48%)/H_2SO_4 (98%) 1:1 (6 ml/100 mg of porphyrin complex) to produce the porphyrinotrifluorosilane monomer (**7**) in CH_2Cl_2 solution. The excess aptes was simultaneously converted to aminopropyltrifluorosilane, which was extracted with aqueous acid. Complex (**7**) exhibited a UV-vis spectrum ($\lambda_{max} = 418$ nm) similar to that of the parent porphyrin (**5**) and of Fe(III)TDCPP itself, indicating that the porphyrin rings were not modified during the preparation.

Complex (**7**) could be used in the functionalization of the oxide surface to give the colloidal composite system TiO_2/Fe(III)–porphyrin. In
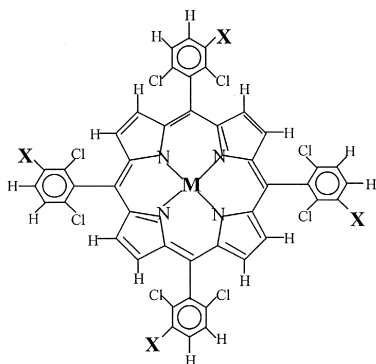
Scheme 1. Synthesis of the modified Fe(III)TDCPP. (**1**) M = H_2, X = H; (**2**) M = H_2, X = SO_2Cl; (**3**) M = H_2, X = SO_3H; (**4**) M = Fe^{3+}, X = SO_3H; (**5**) M = Fe^{3+}, X = SO_2Cl; (**6**) M = Fe^{3+}, X = $SO_2NH(CH_2)_3Si(OEt)_3$; (**7**) M = Fe^{3+}, X = $SO_2NH(CH_2)_3SiF_3$.

fact, when the iron–porphyrin complex (**7**) was added to an alcoholic suspension of colloidal TiO_2, the SiF_3 groups were immediately converted to SiOH by the water molecules present on the oxide surface and the iron–porphyrin complex was covalently linked to TiO_2 (as schematized in Fig. 1) by one or more of its aminopropyl arms. Furthermore, it is also possible that the formation of some dimers or oligomers between the iron–porphyrin complexes bonded on the semiconductor surface. Although, given the low coverage by the complex, this phenomenon should not be extensive.

2.2. Materials

The colloidal composite system $TiO_2/$Fe(III)–porphyrin used has been prepared as described in the previous paragraph. All the organic solvents and substrates employed (MeOH, DMF, CH_2Cl_2, cyclohexane, etc.) were spectroscopic grade reagents and were used without further purification. Cyclohexene was distilled before use.

2.3. Apparatus and methods

Laser flash photolysis experiments were carried out using an Applied Photophysics detection systems coupled with a Continuum Surelite II-10 neodinium YAG laser, equipped with a frequency multiplier (355 nm, 5 ns half-width, 150 mJ). The eventually observed absorbance variations after the flash have been read on a LeCroy 9360 fast digitizing oscilloscope.

Irradiations were carried out with a medium-pressure Hg/Xe lamp, with thermostated cell holder ($22 \pm 1°C$). The desired wavelength interval ($300 < \lambda < 370$ nm) has been selected using a $NiSO_4$ solution (8 g in 10 ml) coupled with a glass cut-off ($T\% = 16$). Product analyses were performed by gas chromatography using a DANI 8521-a equipped with a flame ionization detector using columns packed with Carbowax 20 M 5% on Chromosorb W-AW. The reaction products were identified by comparison of their retention times with those of the authentic samples. Carbon dioxide formed during the experiments has been collected into a solution of $Ba(OH)_2$ (1×10^{-2} M) in sodium silicate (1×10^{-3} M). Then, $BaCO_3$ has been determined by a turbidimetric method using a calibration curve.

The samples were prepared as follows: colloidal TiO_2 (5 mg) was suspended in the chosen medium (3 ml) and an aliquot of iron–porphyrin, corresponding to a concentration of 2×10^{-5} mol dm^{-3}, was added. When needed, the samples were deaerated, bubbling N_2 in it before proceeding with the experiment. For the photocatalytic experiments, the colloidal suspension of TiO_2 added with Carbowax was stationed
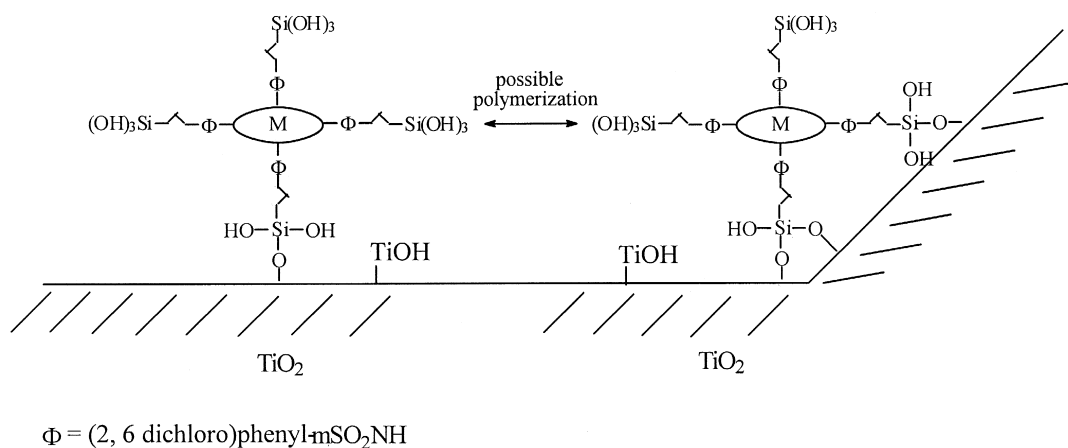

$\Phi = (2, 6 \text{ dichloro})\text{phenyl-}m\text{SO}_2\text{NH}$

Fig. 1. Schematic structure of the composite colloidal system $TiO_2/$Fe(III)–porphyrin.

along a glass sheet (1 cm in width) to form a thin film of colloid; after solvent evaporation, the sheet was put into the oven at 450°C for 30 min. When necessary, its immersion into a functionalized iron–porphyrin solution led to a deposited film of the composite system. The glass sheet so obtained was put into a suitable spectrophotometric cell containing cyclohexane or DMF/CH$_2$Cl$_2$/cyclohexene (4:2:1) mixed solvent to be irradiated in the presence of a saturated atmosphere of O$_2$. Electrochemical experiments were performed with an EG&G potentiostat/galvanostat and EG&G software. Electrodes were prepared by depositing films of TiO$_2$ onto Ti sheets, which were previously etched in concentrated oxalic acid at 80°C. When required, the electrodes were illuminated using a Hanau Q-400 medium-pressure mercury lamp equipped with a filter to cut off light of wavelength $\lambda < 360$ nm. The supporting electrolyte was 0.1 mol $\times$ dm^{-3} NaClO$_4$; a Pt sheet and saturated calomel were used as the counter and reference electrode, respectively.

3. Results and discussion

3.1. Photoredox properties

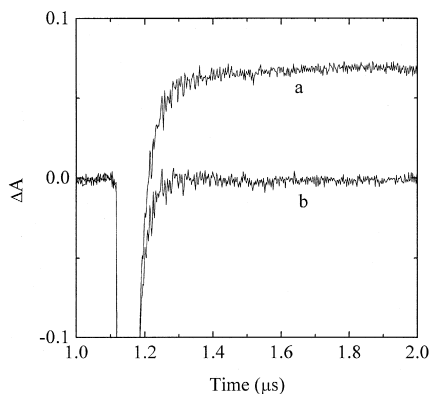In the laser flash photolysis experiments, the excitation wavelength ($\lambda = 355$ nm) was such

Fig. 2. Laser flash photolysis of the colloidal composite system TiO$_2$/Fe(III)–porphyrin dissolved in MeOH (curve a) and in H$_2$O (curve b), in the absence of O$_2$. $\lambda_{exc} = 355$ nm, $\lambda_{anal} = 423$ nm.
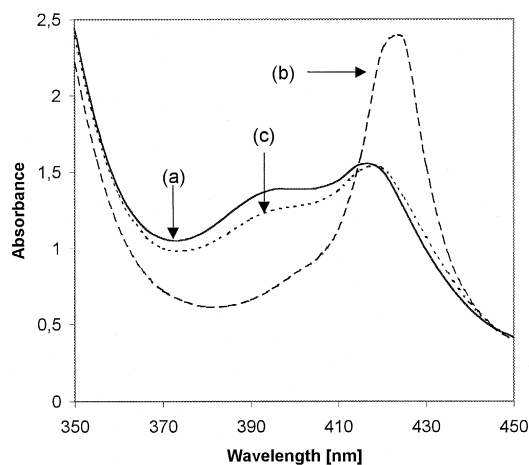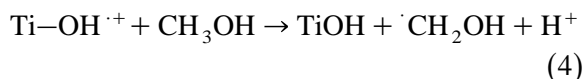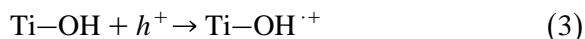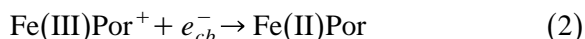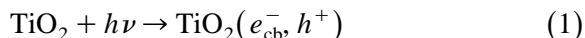

Fig. 3. UV-vis spectra of the colloidal composite system before the flash (curve a), after the flash (curve b), and after the flash and oxygenation of the sample (curve c).

that light was absorbed completely by TiO$_2$, which worked as the photochemical active component of the colloidal composite system TiO$_2$/Fe(III)–porphyrin, while the analysis wavelength ($\lambda = 423$ nm) corresponded to the absorption maximum of the iron–porphyrin complex in its reduced form. Fig. 2 reports the main results obtained: when the composite colloidal system was suspended in MeOH, the flash gave rise to an absorption increase (curve a) indicating the reduction of Fe(III) to Fe(II). Furthermore, its UV-vis spectrum after the flash showed the typical band of reduced iron–porphyrin (Fig. 3, curve b); oxygenation of the sample led to the original spectrum of the oxidized form (curves a and c). Therefore, these results point out that photoexcited TiO$_2$ can work as electron source for the reduction of the iron(III)–porphyrin (Eqs. 1 and 2). Simultaneously, the alcohol can rapidly capture the valence band holes or, alternatively, react with surface OH radicals (Eqs. 3 and 4).

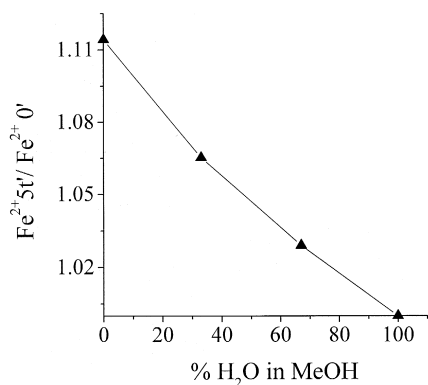$$TiO_2 + h\nu \rightarrow TiO_2(e_{cb}^-, h^+) \qquad (1)$$

$$Fe(III)Por^+ + e_{cb}^- \rightarrow Fe(II)Por \qquad (2)$$

$$Ti{-}OH + h^+ \rightarrow Ti{-}OH^{\cdot+} \qquad (3)$$

$$Ti{-}OH^{\cdot+} + CH_3OH \rightarrow TiOH + {}^{\cdot}CH_2OH + H^+ \qquad (4)$$

Fig. 4. Concentration of Fe(II)–porphyrin formed after 5 min of irradiation $(300 < \lambda < 370$ nm) of the composite colloidal system dissolved in MeOH/H_2O mixed solvents with different composition.

On the other hand, when the composite colloidal system was suspended in water, we did not observe any absorption increase after the flash. Unfortunately, it has not been possible to carry out the experiments in a shorter time scale because of unavoidable light-scattering phenomena by the colloidal suspensions. Continuous irradiation of deaerated composite colloidal system suspensions in various MeOH/H_2O mixtures (Fig. 4) showed that the concentration of reduced iron–porphyrin, produced in the primary photochemical process decreased when the content of water in the mixture increased. The instability of the porphyrin reduced form in water may be due to the fact that, in the absence of alcohol, OH surface radicals can oxidise the reduced porphyrin complex as in Eq. 5.

$$Ti-OH^{\cdot+} + Fe(II)Por \rightarrow TiOH + Fe(III)Por^+ \tag{5}$$
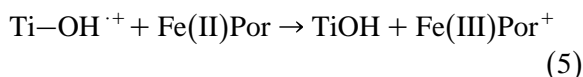
In contrast, in methanol, the capture of OH radicals (or valence band holes) yields CH_2OH radicals with sufficient reducing power to favour the formation of the Fe(II) complex through the following reaction:

$$^{\cdot}CH_2OH + Fe(III)Por^+ \rightarrow Fe(II)Por$$
$$+ CH_2O + H^+ \tag{6}$$
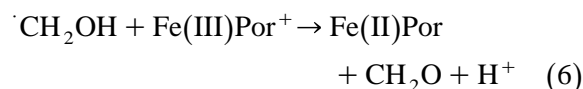
This process would account for the accumulation of Fe(II) in this particular environment. In the following section, we discuss possible additional explanations.

3.2. Photoelectrochemical experiments

We carried out electrochemical experiments with porphyrin-modified TiO_2 photoelectrodes to attempt a further characterization of the nature of the interactions between the composite system and the liquid medium. A comparative behavior of the photocurrents vs. potential curves is given in Fig. 5 for TiO_2 and porphyrin–TiO_2 electrodes in aqueous solution and in DMF/H_2O mixtures. It is clear in this figure that only in the case of the porphyrin–TiO_2/H_2O system does one observe a clearly distinct behavior. There is, in fact, a sensible shift of the photocurrent onset to higher positive potentials, which indicates that electron–hole recombination is prevailing at potentials approaching the flat band value. Accordingly, the value of flat band potential derived from Mott–Schottky plots was -0.3V for porphyrin–TiO_2/H_2O and -0.4V for the other systems. The data are in agreement with those discussed above on the impossibility to reveal the presence of the Fe(II)–porphyrin in H_2O.
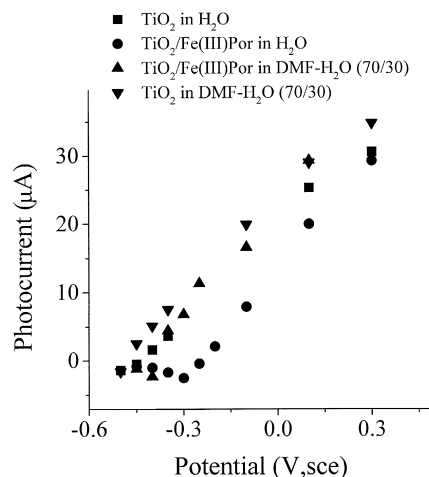

Fig. 5. Photocurrent values vs. applied potential for colloidal TiO_2 deposited on a Ti electrode in H_2O and in H_2O/DMF (30:70) both in the absence and in the presence of the Fe(III)–porphyrin complex.

The photocurrents plot of Fig. 5 does not indicate any significant oxidation of DMF. Instead, one important point to note is the ability of DMF (shared by CH_3OH) to coordinate to the axial positions of the Fe(III)–porphyrin. We then think that a possible explanation of the observed phenomena is due to the fact that the coordinating organic solvent tends to change the orientation of the porphyrin in such a way as to decrease the degree of its interaction with the oxide surface. In other words, in an aqueous medium, in the absence of strongly bonded axial ligands, the linked porphyrin would lie closer to the surface and an interaction with surface hydroxyl groups would be easier than in the case of a strongly coordinating medium. This explanation is in agreement with the mechanism proposed for aminopropyl surface immobilized redox centers [30] in general, and porphyrins in particular [11], where electron transfer occurs via a ''floppy'' chain folding model.

3.3. Photocatalytic properties

The results so far discussed provide evidence, at least in organic media, of redox processes occurring between the iron–porphyrin complex and the photoexcited TiO_2. This fact arose our interest; in particular, we wanted to verify the behaviour of the composite system in the photooxidation of cyclohexane, because it is a simple alkane, which has already been tested with a variety of photocatalysts [21–26] and also because its oxidation products are important intermediates in many industrial processes such as,

for example, the production of adipic acid and Nylon 6.

It has not been possible to perform the cyclohexane photooxidation using the colloidal system itself because it could not be suspended in any medium containing the hydrocarbon. For this reason, we decided to use films obtained by depositing the colloid on a glass sheet, which has been immersed into neat cyclohexane.

Table 1 shows that the presence of the iron–porphyrin complex significantly increases the photocatalytic efficiency with respect to colloidal TiO_2 alone, since the overall concentration of the oxidation products grows by about 50%. In addition, the iron–porphyrin changes the selectivity in the formation of monooxygenated products, increasing the cyclohexanol/cyclohexanone ratio.

We observe here for the first time that surface derivatization of TiO_2 leads to an improvement in the photocatalytic oxidation of hydrocarbons. The new procedure adopted in the functionalization of the surface is probably the main reason for the comparatively higher efficiency of the composite catalyst described herein. In fact, in our previous work, we used a two-step method where the surface was first treated with aminopropylsilane, and then the porphyrin complex grafted thereon. The first step dramatically inactivates the surface, while the photocatalytic activity is 35% regenerated when the porphyrin is bonded to the surface [21,22]. The procedure adopted in this work apparently allows a better sites synergy, with the iron–porphyrin, providing alternative path-

Table 1
Photocatalytic properties ($300 < \lambda_{exc} < 370$ nm) of TiO_2 and of the composite system TiO_2/Fe(III)–porphyrin as films deposited on glass sheets in the oxidation of cyclohexane

Photocatalytic system	$[C_6H_{10}O + C_6H_{11}OH]$[a]	$[CO_2]$[a]	$[C_6H_{11}OH]/ [C_6H_{10}O]$	[Monooxygenated products]/$[CO_2]$
TiO_2[b]	26	7.9	0.15	3.2
TiO_2/Fe(III)–porphyrin[b]	44	8.8	0.37	5

[a]Concentrations ($\times 10^4$ mol dm^{-3}). Reported values are $\pm 5\%$.
[b]Medium: 3 ml of neat cyclohexane. Irradiation time 360′.

ways in the known reaction mechanism of photoexcited TiO_2 [23].

Concerning the selectivity of the system for the oxidation processes under examination, it is necessary to point out that the total degradation of the hydrocarbons leads to CO_2 formation. When this is counted among the products, we can conclude that in all cases, the porphyrin derivatization of the oxide improves the overall selectivity of the processes.

Another important issue is the catalyst stability. In this respect, we noted that during the photocatalytic experiments, the iron–porphyrin complex undergoes a slow degradation. It has been possible to evaluate a turnover number (ratio between the moles of photooxidized cyclohexane and the moles of degraded iron–porphyrin complex) equal to 12 000. This value

indicates that heterogenization on TiO_2 increases the porphyrin stability by two orders of magnitude with respect to the same experiments where the complex was used in solution in the absence of TiO_2 [31–33].

Scheme 2 shows some possible reaction pathways explaining the effect of the iron–porphyrin on the photocatalytic efficiency of TiO_2 as well as on the observed change in the selectivity of cyclohexanol formation (Table 1). Route A concerns the formation of intermediates and stable oxidation products at the semiconductor surface independently of surface functionalization. The hydrocarbon (RH) is oxidized to a radical species by the photogenerated holes in analogy with the above discussion for methanol oxidation. The reaction between $R^\bullet$ and surface OH radicals leads to the formation of the cyclohex-
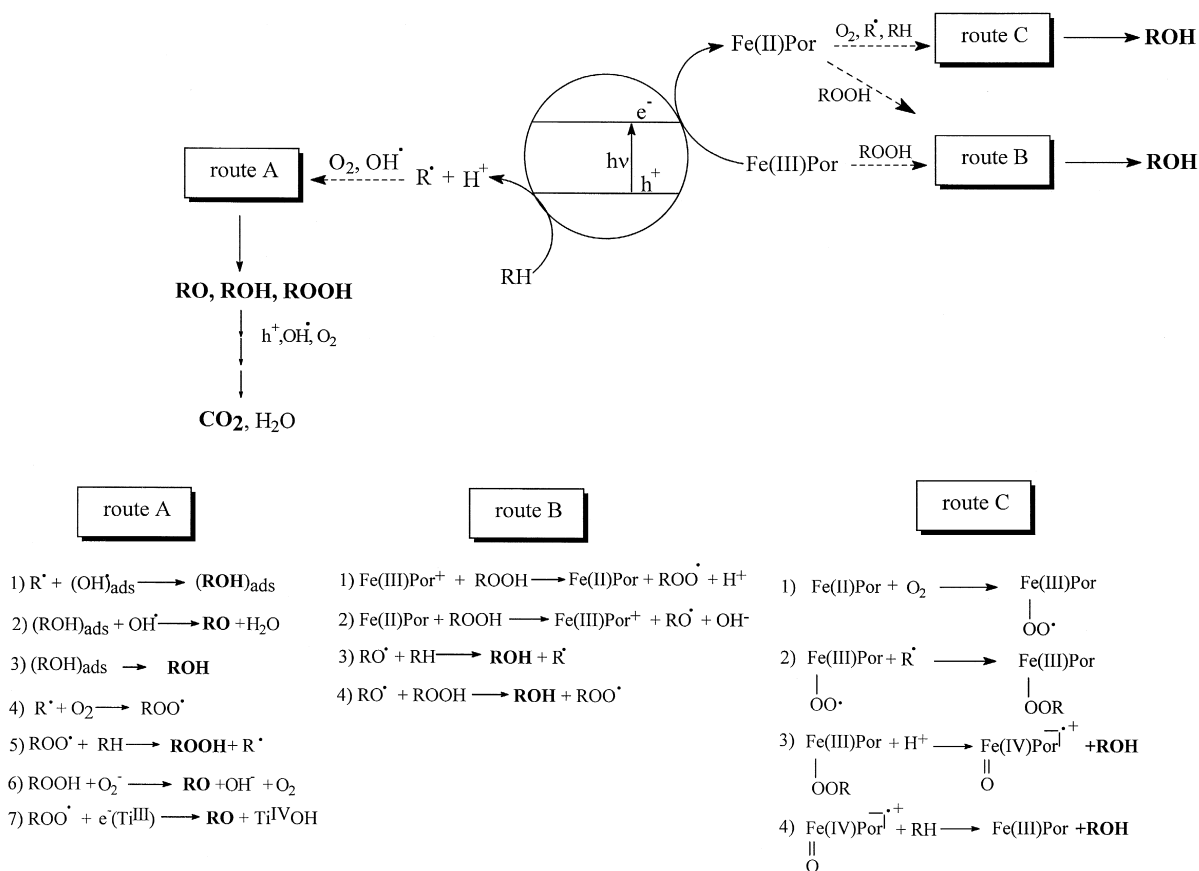
Scheme 2. Schematic representation of the proposed photooxidation reaction mechanism.

anol, which can be efficiently oxidized to cyclo-hexanone before its desorption [23]. The direct reaction of R˙ with O_2 would yield peroxo species, ROO˙ and ROOH, which could eventually form the ketone. Subsequent oxidation reactions lead to the total degradation of the organic substrate.

Although these species are formed irrespective of whether the surface is modified or not, there could still be an influence of the iron–porphyrin complex on how they evolve. For example, reaction 5 of route A can be inhibited because the peroxide species can react with the porphyrin complex, both in its ferric and ferrous form, leading exclusively to cyclohexanol (route B). Based on literature data [34], these reactions should be particularly relevant when a halo-genated iron–porphyrin is involved.

Other possible reactions, which can explain the high yield in alcohol among the products are represented by Eqs. 1–4 of route C. These take place as a consequence of the photoinduced reduction of the ferric porphyrin (Eq. 2) and lead to the reductive activation of O_2. On the other hand, the reaction of the photogenerated R˙ with the Fe(II)–porphyrin in the presence of O_2 can give a species of the type Fe(III)-OOR [32,33]. As previously proposed in the catalytic cycle of 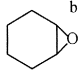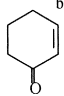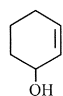*P*-450 [35,36], this species undergoes a heterolytic cleavage of its peroxidic bond whereby forming intermediate species, which are able to hydroxylate alkanes.

In view of our continuing interest in hydrocarbon oxidation, we tested the TiO_2/Fe(III)–porphyrin composite system also in the photo-oxidation of cyclohexene, as model molecule of alkenes. However, it has not been possible to perform the oxidation experiments immersing the glass supported films in neat cyclohexene, because of the noteworthy thermal reactivity of this substrate towards autooxidation processes. For this reason, Table 2 reports the results obtained using a mixture of solvents, where cyclohexene was the minor component.

As noticed for cyclohexane, the presence of the iron–porphyrin significantly increases the photocatalytic efficiency of the system. However, we failed to observe an effect of the porphyrin on the monooxygenation products distribution. These results are possibly explained by the fact although the oxidation cyclohexene benefits from a higher amount of dioxygen activated species, it is too reactive to preferably follow some porphyrin-mediated reaction pathways, and products are mainly formed via autooxidation processes. It is important to note, however, that in this case, too, we observe an increase in selectivity with respect to unmodi-

Table 2
Photocatalytic properties ($300 < \lambda_{exc} < 370$ nm) of TiO_2 and of the composite system TiO_2/Fe(III)–porphyrin as films deposited on glass sheets in the oxidation of cyclohexene

Photocatalytic system	Total amount [b]	(epoxide) [b]	(enone) [b]	(enol OH) [b]	CO_2 [b]	[Monooxygenated products]/[CO_2]
TiO_2 [a]	11	0.4	8.1	2.2	0.3	37
TiO_2/Fe(III)-porphyrin [a]	31	1.4	22	7.1	0.5	62

[a] Medium: 3 ml of DMF/CH_2Cl_2/cyclohexene (4:2:1). Irradiation time 180′.
[b] Concentrations ($\times 10^4$ mol dm^{-3}). Reported values are $\pm 5\%$.

fied TiO_2 when the ratio of the amount of monooxygenation products vs. CO_2 is considered (Table 2).

4. Conclusions

The present work discusses the photochemical behavior of nanocrystalline TiO_2, which is modified by a Fe(III)–porphyrin linked to the surface via a silane bond. With respect to existing literature on derivatization methods, we adopted a new procedure whereby the complex rather than the surface contains the silane functional group.

The nature of the solvent has an important role in determining the accumulation of the porphyrin reduced form in the absence of oxygen. Assuming a ''floppy'' chain folding model for the bonded porphyrin, this is explained in terms of a coordination of solvent molecules to the porphyrin metal center, which results in a re-orientation of the complex so as to decrease its interaction with the surface. The fact that the results can be well explained on the basis of this model, seems to exclude significant contributions of porphyrin dimerization or oligomerization phenomena on the surface, since this would create less flexible structures.

The photocatalytic properties of the system were assessed in the processes of monooxygenation of cyclohexane and cyclohexene with molecular oxygen. The presence of iron–porphyrin causes an important increase of the photocatalytic efficiency with respect to the unmodified nanocrystalline TiO_2 alone, since the overall concentration of the oxidation products increases by a factor of 2 in the former case. This is in contrast with what was observed with previously described iron–porphyrin/TiO_2 photocatalysts that were prepared by a different procedure of functionalization of TiO_2 surface.

Moreover, we find out a decrease in CO_2 formation, making the composite system a better photocatalyst for synthesis processes than unmodified TiO_2. In the case of cyclohexane,

the iron–porphyrin complex also changes the selectivity of the process for the monooxygenation products formation, increasing the alcohol to ketone ratio. The ability of the iron–porphyrin complex to tune the high oxidation power of the semiconductor is an important characteristic of the composite system, especially when the interest is focused on synthesis rather than on detoxification processes.

References

[1] R. Murray (Ed.), Molecular Design of Electrode Surfaces, Wiley, New York, 1992.
[2] P. Allongue, in: B.E. Conway, J.O'M. Bockris, R.E. White (Eds.), Modern Aspects of Electrochemistry vol. 23 Plenum Press, New York, 1992.
[3] A.J. McEvoy, M. Grätzel, Sol. Energy Mater. Sol. Cells 32 (1994) 221.
[4] R. Amadelli, R. Argazzi, C.A. Bignozzi, F. Scandola, J. Am. Chem. Soc. 112 (1990) 7099.
[5] B. O'Regan, M. Grätzel, Nature 353 (1991) 737.
[6] G.J. Meyer (Ed.), Molecular Level Artificial Photosynthetic Materials, Progress in Inorganic Chemistry Series vol. 44 Wiley, New York, 1997, and references therein.
[7] D.F. Untereker, J.C. Lennox, L.M. Wier, P.R. Moses, R.W. Murray, J. Electroanal. Chem. 81 (1977) 309.
[8] I. Haller, J. Am. Chem. Soc. 100 (1978) 8050.
[9] H.O. Flinkea, R.W. Murray, J. Phys. Chem. 83 (1979) 353.
[10] M. Tomkiewicz, J. Electrochem. Soc. 127 (1980) 1518.
[11] M. Fujihira, T. Kubota, T. Osa, J. Electroanal. Chem. 119 (1981) 379.
[12] Kabir-Ud-Din, C. Owen, M.A. Fox, J. Phys. Chem. 85 (1981) 1679.
[13] H.O. Flinkea, R. Vithanage, J. Phys. Chem. 86 (1982) 362.
[14] P. Kamat, M.A. Fox, J. Phys. Chem. 87 (1983) 59.
[15] R. Vithanage, H.O. Flinkea, J. Electrochem. Soc. (1984) 799.
[16] T.R. Hayes, J.F. Evans, J. Phys. Chem. 88 (1984) 1963.
[17] A.P. Hong, D.W. Bahneman, M.R. Hoffmann, J. Phys. Chem. 91 (1987) 2109.
[18] A.P. Hong, D.W. Bahneman, M.R. Hoffmann, J. Phys. Chem. 91 (1987) 6245.
[19] A.P. Hong, S.D. Scott, M.R. Hoffmann, Environ. Sci. Technol. 23 (1989) 533.
[20] W.G. Becker, M.M. Truong, C.C. Ai, N.N. Hamel, J. Phys. Chem. 93 (1989) 4882.
[21] R. Amadelli, M. Bregola, E. Polo, V. Carassiti, A. Maldotti, J. Chem. Soc. Chem. Comm. (1992) 1355.
[22] E. Polo, R. Amadelli, V. Carassiti, A. Maldotti, in: M. Guisnet, J. Barbier, J. Barrault, C. Bouchoule, D. Duprez, G. Pérot, C. Montassier (Eds.), Heterogeneous Catalysis and Fine Chemicals III, Elsevier, The Netherlands, 1993, p. 409.
[23] P. Boarini, V. Carassiti, A. Maldotti, R. Amadelli, Langmuir 14 (1998) 2080, and references therein.

[24] A. Maldotti, A. Molinari, P. Bergamini, R. Amadelli, P. Battioni, D. Mansuy, J. Mol. Catal. A: Chemical 113 (1996) 147.

[25] A. Maldotti, A. Molinari, R. Argazzi, R. Amadelli, P. Battioni, D. Mansuy, J. Mol. Catal. A: Chemical 114 (1996) 141.

[26] A. Molinari, A. Maldotti, R. Amadelli, A. Sgobino, V. Carassiti, Inorg. Chim. Acta 272 (1998) 197.

[27] B. O'Regan, J. Moser, M. Anderson, M. Grätzel, J. Phys. Chem. 94 (1990) 8720.

[28] P. Battioni, E. Cardin, M. Louloudi, B. Schollhorn, G.A. Spyroulias, D. Mansuy, T.G. Traylor, Chem. Commun. (1996) 2037.

[29] J.S. Lindsey, H.C. Hsu, I.C. Schreiman, Tetrahedron Lett. 27 (1986) 4969.

[30] P.R. Moses, R.W. Murray, J. Am. Chem. Soc. 98 (1976) 7435.

[31] P. Battioni, J.F. Bartoli, D. Mansuy, Y.S. Byun, T.G. Traylor, J. Chem. Soc. Chem. Comm. (1992) 1051.

[32] A. Maldotti, C. Bartocci, G. Varani, A. Molinari, P. Battioni, D. Mansuy, Inorg. Chem. 35 (1996) 1126.

[33] A. Maldotti, C. Bartocci, R. Amadelli, E. Polo, P. Battioni, D. Mansuy, J. Chem. Soc. Chem. Comm. (1991) 1487.

[34] M.W. Grinstaff, M.G. Hill, J.A. Labinger, H.B. Gray, Science 264 (1994) 1311.

[35] M. Sono, M.P. Roach, E.D. Coulter, J.H. Dawson, Chem. Rev. 96 (1996) 2841, and references therein.

[36] J.T. Groves, Y.Z. Han, in: P.R. Ortiz de Montellano (Ed.), Cytochrome *P*450, Structure, Mechanism and Biochemistry, 2nd edn., Plenum Press, New York, 1995.